JD
SS

The Observation, Measurement and Modeling of Artificial Light Pollution

John C. Barentine[1,2,*] and Bryan O. Boulanger[3]

[1] International Dark-Sky Association, 3223 N. First Avenue, Tucson, AZ 85719 USA; john@darksky.org
[2] Consortium for Dark Sky Studies, University of Utah, 375 S 1530 E, RM 235 ARCH, Salt Lake City, Utah 84112-0730 USA
[3] Civil and Environmental Engineering Department, Ohio Northern University, Biggs 108, 525 S. Main Street, Ada, OH 45810 USA; b-boulanger@onu.edu
* Correspondence: john@darksky.org; Tel.: +1-520-347-6363

Version October 16, 2019 submitted to JDSS

Abstract: Artificial light at night (ALAN) has become a ubiquitous environmental pollutant known to reduce visibility of the night sky and harm the integrity of ecosystems. ALAN additionally has an impact on public safety, energy security, and climate change. Approximately eighty percent of the world's population currently live under light-polluted night skies, and both the artificially illuminated land area of the Earth and the brightness of illuminated areas are increasing at a global average of twice the rate of human population growth. Although there is abundant evidence suggesting that light pollution is a major environmental challenge, the production and consumption of ALAN is tied in complex ways to human development goals. To find the best ways of confronting and ameliorating the problem of light pollution, we must first quantify the presence of ALAN on multiple spatial scales and model its behavior in the environment. In this paper, we review various measurement approaches of ALAN, as well as models constructed to account for its observed properties. These measurements and models may contribute to outdoor lighting design, conservation, and public policy interventions whose goals are to mitigate light pollution to the greatest practical extent while providing reasonably for the legitimate human uses of ALAN.

Keywords: light pollution; skyglow; remote sensing; numerical modeling

1. Introduction and Motivation

Pollution from artificial light at night (ALAN) is an issue of contemporary global concern. For most of Earth's history, life evolved in the context of natural cycles of light and dark. While nighttime darkness is natural, it is important to point out that natural darkness is not without natural sources of light. In fact, there are many sources of natural light at night that have ecological and biological functions. Sources of natural light at night include astronomical light of the Moon, stars and planets; atmospheric sources like airglow and aurorae; and ground-based emissions from wildfire, lightning and bioluminescence. However, in many places around the globe, those natural sources of light at night have been displaced by human-caused, often overpowering, and mostly electric light. ALAN, therefore, represents a novel (and largely unknown) challenge to biological systems unable to quickly adapt to rapidly changing conditions and ecological landscapes where its impact may not be immediately recognized.

Initial realization of the broad environmental harm associated with "light pollution," as well as the first instances of the use of that term, came in the late 1960s. [1] However, the first hints of adverse effects of ALAN were reported by astronomers early in the nineteenth century, when the starry quality of night skies

over European cities began to degrade as a result of the installation of the public outdoor lighting systems powered by the combustion of coal gas. [2] The brightening of cities accelerated beginning in the 1880s after the introduction of electric light. [3] Soon after biologists began to report the often fatal attraction of species to the new lights. [4–6] Now, ALAN is present in the outdoor environment over a large fraction of the globe. [7] Averaged across the world, both the rate at which new indications of ALAN are appearing on Earth and the amount of light radiated in the upward direction at night exceed two percent per year, with individual countries exceeding 10 percent annual growth in both quantities. [8] Surprisingly large variations in ALAN use are seen even within particular countries. [9]

Much of the concern about ALAN in outdoor settings has to do with its propensity to form skyglow, which is light received at the surface of the Earth from upward-directed sources on the ground after one or more scattering events in the atmosphere. Light sources whose spectral power distributions (SPDs) are strong in short-wavelength ($\leq$ 500 nm) emissions are a particular concern from an environmental perspective. Small-particle scattering in the Earth's atmosphere increases the reach and intensity of skyglow away from the sources where it originates, with a strong bias toward shorter wavelengths. [10–12] ALAN exposure from both direct illumination and skyglow is known to impact a vast array of species on Earth. To date, virtually every organism studied has shown some response to ALAN, and nearly all react in ways that negatively impact both individuals and entire populations. Observed impacts are reported among birds, [13–16] fishes, [17,18] mammals, [19–21] reptiles, [22–24] invertebrates, [25–28] and plants. [29–31]

Although most humans receive the bulk of their ALAN exposure from sources in indoor environments, the effects of ALAN on humans and human cultures from outdoor sources should be considered. The causal relationship between ALAN exposure and human health and wellbeing is a controversial subject far from clear definition; there are, however, strong indications that ALAN has some effects on human health. Exposure to short-wavelength light entrains the circadian rhythm that governs everything from the timing of hormone secretion to the sleep-wake cycle. [32] Exposure to ALAN at inappropriate times during this cycle delays or suppresses altogether the onset of the secretion of melatonin, [33] a potent antioxidant known to interact with the immune system. [34] The resulting disruption of the circadian rhythm causes epigenetic changes that may lead to metabolic disorders and cancer morbidity. [35]

Because ALAN is associated with adverse effects recognizable by different disciplines, understanding ALAN occurrence, spatial and spectral distributions, and exposure is an important transdisciplinary aim made all the more important given the rapid advance of solid-state lighting in the past decade. The widespread adoption of energy-efficient white light-emitting diode (LED) technology in particular has lowered the cost of consuming ALAN in both indoor and outdoor settings. While LED technology offers potential environmental benefits associated with lowered electricity consumption and carbon emissions, the impact of white LEDs on ALAN presents novel challenges to reducing the observed impacts of light pollution. [8]

Despite the challenges, reducing the impact of ALAN is achievable. While simply shutting off ALAN would alleviate its negative consequences, this approach is neither practical nor responsive to the many social benefits of ALAN. Rather, a balanced approach is warranted that seeks to reduce the harms associated with ALAN while providing outdoor lighting in ways responsive to human needs. The desired outcome of reducing ALAN will require a mixture of policy, technology, science, and design solutions that depend upon our collective ability to assess and monitor ALAN. Over the past two decades advances in remote sensing, skyglow measurements, and radiative transfer modeling have all helped inform decision making regarding both the impacts of ALAN and a growing desire to mitigate them. Direct measurements elucidate the extent and characteristics of the problem, while modeling allows for better developed understanding of the factors influencing light pollution and what can be done to further reduce its prevalence. This overview follows the development of measurements, monitoring, and modeling, and concludes with a look toward the future needs of the research community.

2. Measurements and Modeling

Fundamentally, measuring ALAN is accomplished by sensing light using established radiometric and/or photometric methods. Radiometry measures electromagnetic radiation across the complete spectrum, while photometry is a subfield of radiometry that scales measurements to the visual perception of the human eye. Radiometric methods are generally used to characterize and quantify ALAN for purposes of remote sensing, while skyglow and lighting design measurements have generally relied upon photometric methods. Remote sensing involves measurements of upward radiance generally taken at large distances from the light source. Upward radiance is the radiant flux from all sources of light, whether emitting directly or indirectly, in some particular direction that is received by the projected area of a given surface per unit solid angle.

Skyglow measurements involve the indirect detection of light at generally small distances from the source after it scatters through the Earth's atmosphere and is redirected to the ground. Skyglow is typically characterized by measurements of luminance, which is the luminous intensity per unit area of light traveling in a given direction. Light measurements seeking to characterize light for ALAN and/or lighting design purposes measure the luminance and/or illuminance (luminous flux incident on a surface). Additionally, by measuring both the wavelength and amplitude of light using a spectroradiometer or spectrophotometer, the spectral composition and color of light may be reported depending upon the application.

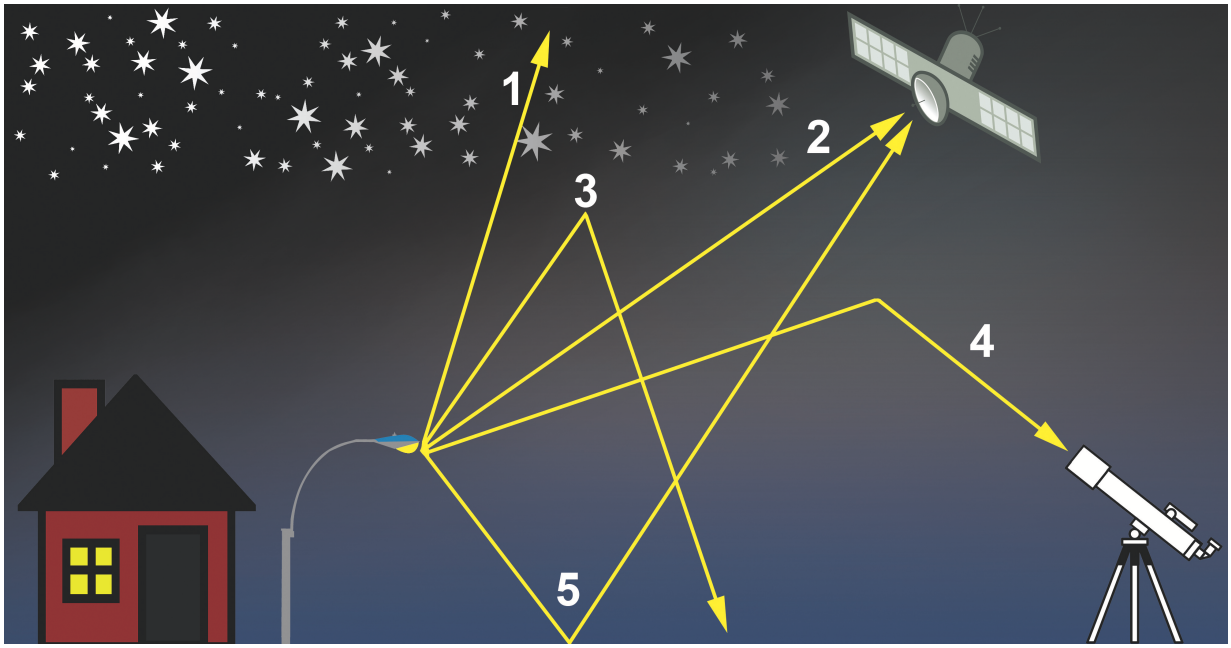

Figure 1. A cartoon diagram showing several possible paths for a light ray emitted by a ground-based source. Refer to the main text for an explanation of the numbers. Not all possible paths taken by rays originating at the source are shown.

Figure 1 depicts how light is propagated from source to observer for measurements. The source, represented by the poorly shielded street light at left, emits light in many different directions. Some of the light rays ("1") are directed into the sky and travel completely through Earth's atmosphere without encountering any scatterers. Of these rays, a few ("2") will be detected by aircraft, satellites, or other platforms above the ground. In other cases ("3"), rays undergo single-order scattering from molecules and aerosols in the atmosphere, giving rise to skyglow ("4"). Lastly, rays directed initially toward the ground can experience reflection from surfaces whose albedo may be high enough to cause their redirection

upward (“5”). Multiple-order scattering, not illustrated in the figure, may result in upward-directed light either escaping the atmosphere or being redirected toward the ground (from cloud cover, for example).

2.1. Remote Sensing Measurements

Remote sensing for ALAN measurements relies on existing satellite-, aircraft-, and spacecraft-based sensor platforms. These observations can be used to derive a wealth of information about human activity, such as the distribution of human settlements, [36] indicators of economic development status, [37, 38] rates of regional and national electric power consumption, [39–41] the presence of human conflict (Figure 2), [42–44] disaster relief needs and progress, [45–47] disease epidemiology, [48] natural resource management, [49] and even to assess the state of overall human wellbeing. [50] Further applications include monitoring impacts of ground-based light sources on protected areas, [51–54] and measuring various atmospheric characteristics, [55–57] including greenhouse gas emissions. [58]

While the earliest use of satellites for observing ALAN likely took place during classified missions of the U.S. Department of Defense Meteorological Satellite Program (DMSP) in the 1960s, the earliest recorded available images of ALAN from DMSP platforms date to 1972. [59] DMSP data have been regularly available to the public since 1992. The images are created using DMSP’s Operational Linescan System (OLS) that provides radiance measurements on a relative scale rather than an absolute value (such as W m-2). Individual DMSP satellites equipped with OLS sensors continue to observe the visual spectrum with approximately 2.7-kilometer resolution on the ground. DMSP-OLS data were used to create the World Atlas of the Artificial Night Sky Brightness, the first truly global view of the spatial distribution of ALAN on Earth. [60] However, the coarse spatial resolution and known problems with the absolute calibration of DMSP-OLS images complicate the interpretation of the data. [61–63]

Higher-resolution data sources for observing and quantifying ALAN arrived in 2011 with the launch of the Suomi National Polar-Orbiting Partnership equipped with the Visible Infrared Imaging Radiometer Suite (VIIRS). VIIRS is a “whiskbroom” scanning radiometer used to generate imagery of the Earth’s clouds, atmosphere, oceans and land surfaces at optical and near-infrared wavelengths. [64,65] One of the VIIRS imaging passbands is the Day-Night Band (DNB), which is capable of imaging nighttime terrestrial light emissions at wavelengths between 500 and 900 nm to a nominal radiance limit of 3 nW cm-2 sr-1, allowing for comparison of ALAN geospatially and temporally. [66,67] VIIRS-DNB allows for resolution down to 750 m, and pixels representing brighter anthropogenic light sources are observed to be stable to within 20 percent of the mean over timescales of several years. [68] Due to their global coverage, radiometric precision and temporal stability, VIIRS-DNB data were used to update the World Atlas of the Artificial Night Sky Brightness in 2016 [7] and to inform models of night sky brightness. [69] An effort has been made to cross-calibrate DMSP-OLS and VIIRS-DNB data in order to provide temporal continuity between historical and contemporary measurements. [70] However, a known limitation of these data is the lower cutoff of the wavelength range to which the VIIRS detector is sensitive, limiting what can be inferred concerning short-wavelength light sources within the data set. [71]

In addition to the larger DMSP-OLS and VIIRS-DNB platforms, current [72–77] and proposed [78–80] small satellite and cubesat missions capable of resolving ALAN sources at resolutions down to 100 m are beginning to provide data. High-resolution imagery is also being produced by fixed-wing aircraft, [81–83] drones, [84] and weather balloons, [85] as well as by astronauts aboard the International Space Station. [86–88] The imagery is both beautiful and eye-opening in its resolution abilities (Figure 3).

2.2. Ground-Based Measurements

Quantifying the amount and extent of light pollution from ground-based platforms serves multiple purposes: it allows for environmental impact assessments and field validation of models while

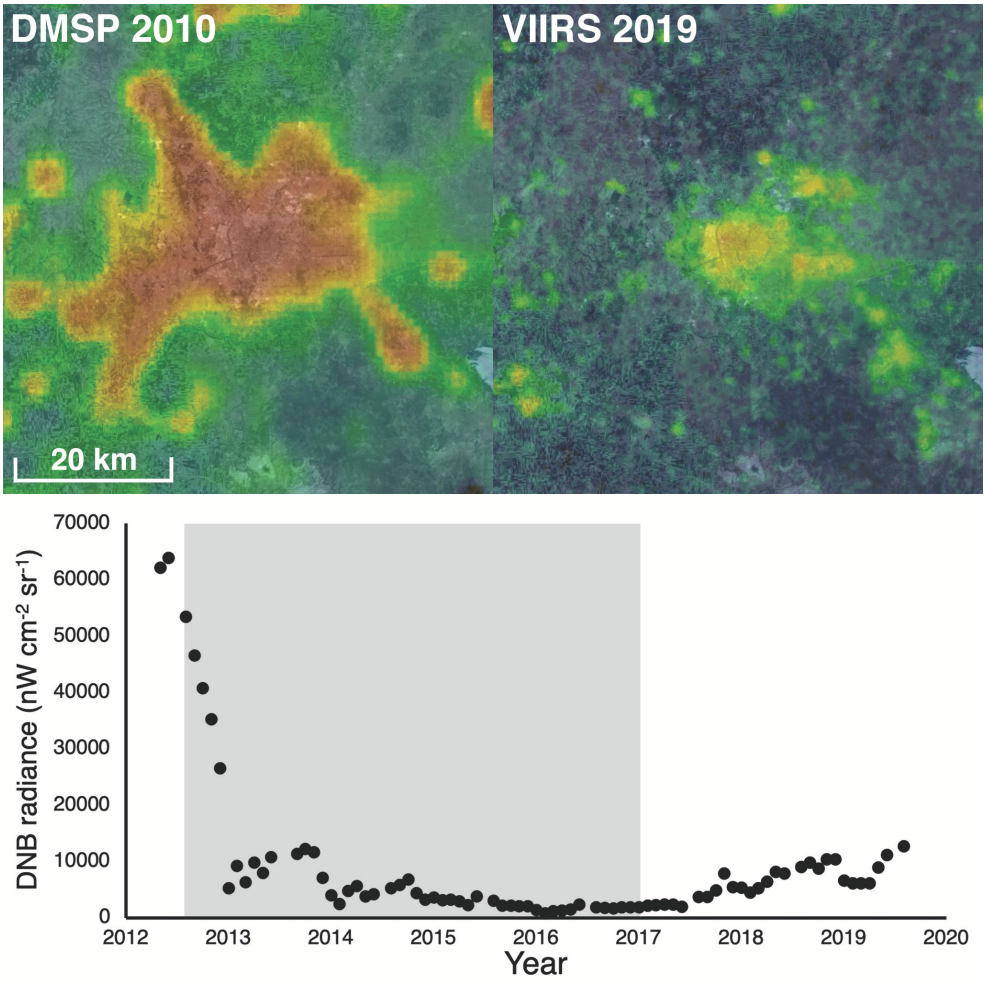

Figure 2. Changes in upward radiance measurements of nighttime light emissions from the city of Aleppo, Syria, during the Syrian Civil War as seen by two Earth-orbiting satellite platforms. Top left: 2010 Defense Meteorological Program Operational Linescan System (DMSP-OLS) annual cloud-free radiance map obtained by the DMSP F18 satellite showing the largest pre-war extent of Aleppo's light emissions. False colors signify radiances in digital numbers from 9 (blue) to 63 (red). Top right: March 2019 Suomi National Polar-Orbiting Partnership Visible Infrared Imaging Radiometer Suite Day-Night Band (VIIRS-DNB) monthly cloud-free radiance map; false colors are radiances from 0.2 nW cm^{-2} sr^{-1} pix^{-1} (blue) to 60 nW cm^{-2} sr^{-1} pix^{-1} (red). Both images are overlaid on Google Maps daytime aerial imagery. Bottom: Summed monthly VIIRS-Day Night Band (DNB) radiances since the launch of Suomi NPP in an 880 km^2 polygon corresponding to the 2010 DMSP-OLS night lights extent around Aleppo. The gray shaded area corresponds to the time period covering the Battle of Aleppo (19 July 2012 – 22 December 2016) during which much of the city's infrastructure was destroyed. (Background map copyright 2019 Google, Landsat/Copernicus/TerraMetrics, used with permission.)

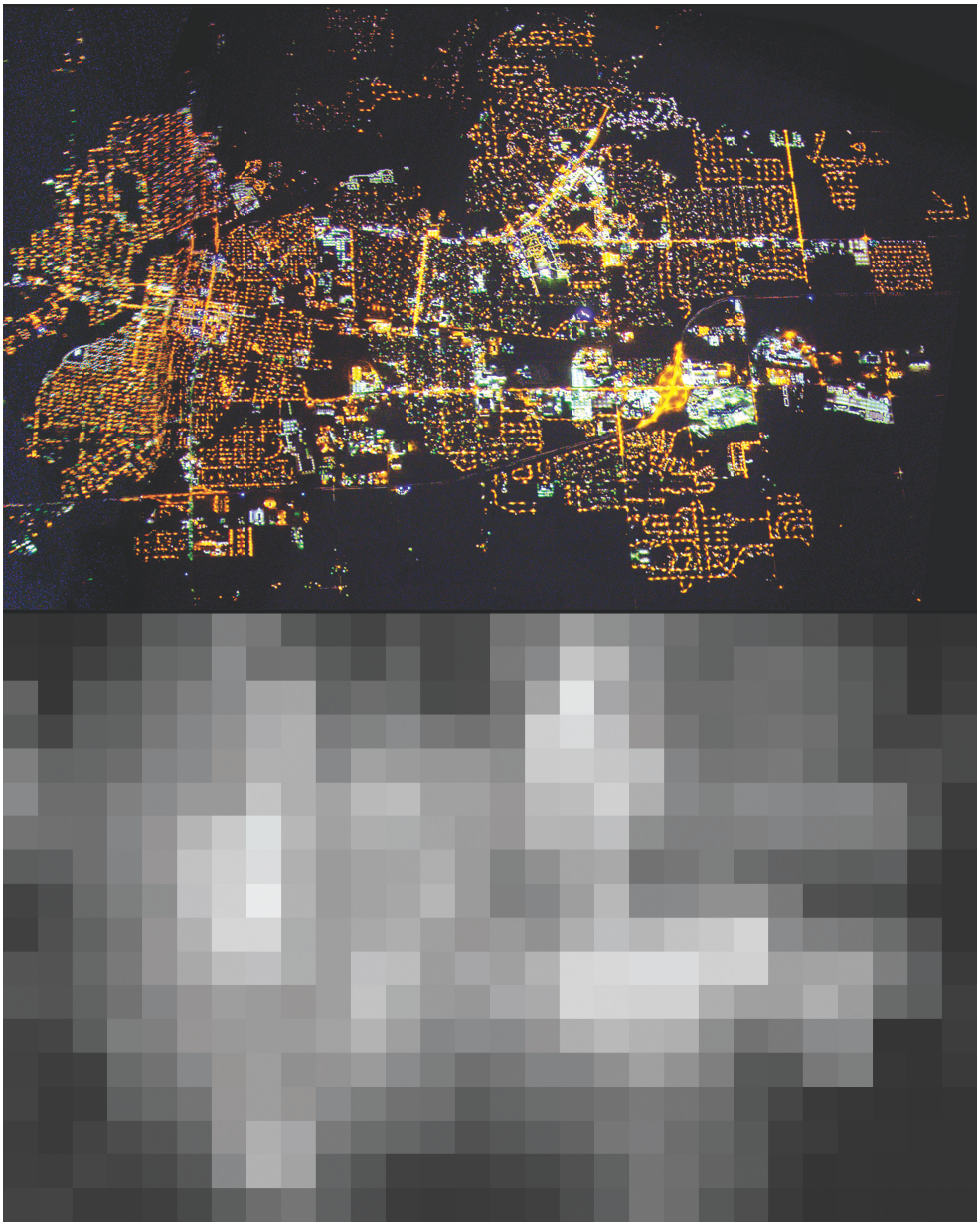

Figure 3. Nighttime imagery of the city of Kankakee, Illinois, (population 26,000) comparing the spatial and spectral resolution capabilities of two remote sensing platforms. The upper panel is an RGB color composite image obtained on 28 April 2019 by cameras aboard the Adler Planetarium NITELite balloon at an altitude of 24 km. [85] The image has dimensions of 10 km by 6 km at a native resolution of $\sim$7 m pix^{-1}, and is oriented with north at right and west at top. It is neither radiance calibrated nor georectified. The lower panel shows the average nightly VIIRS-DNB broadband radiances for Kankakee during the month of April 2018 with the same dimensions and orientation. The DNB image has been reprojected onto a grid with a spatial resolution of $\sim$350 m pix^{-1}.

simultaneously enabling long-term site monitoring. Furthermore, ground-based observations of skyglow are essential to fully understanding remote sensing measurements, and in particular, their limitations. This is even more important now in a world in which the spectral power distribution of the night sky is changing as humanity continues its transition away from earlier lighting technologies and toward solid-state lighting. [89] Because ALAN is not static in either distribution or spectrum, improvements to sensing techniques pose a problem as later data are not usually comparable in a direct way to archival data.

There are several techniques for quantifying the brightness of the night sky, each with their own set of benefits and drawbacks. [90] Broadly these techniques fall into two divisions based on whether or not spectral information is generated. These are different forms of broadband and spectrally resolved measurements consisting of both photometry and imaging, whether in single (1-D) or multiple spatial channels (2-D).

Single channel radiance detectors have become common field measurement tools since the introduction of the Sky Quality Meter (SQM), [91] manufactured commercially by Unihedron of Ontario, Canada, in the early 2000s. The SQM is an inexpensive, portable, networkable, frequency-counting photometer with temperature compensation. It has been shown to be precise (2σ standard error of $\pm$0.028 mag arcsec^{-2}), [91] linear to <3% over 12 magnitudes, [91] intercomparable to $\pm$15%, [92] temperature stable to <7% between 15-35°C and during temperature changes of -33°C h^{-1} and +70°C $^{-1}$, [93] and photometrically stable to <10% year to year in long-term operation. [94] The native SQM photometric passband encompasses a broad range of wavelengths from about 370-700 nm. [91] The wide availability and low cost of devices like the SQM has enabled the deployment of small- to medium-scale networks of these devices for regional sky brightness monitoring. [95] For example, Pun and So characterized skyglow over Hong Kong from 199 sites using autonomous, data-logging SQMs transmitting data via the 3G commercial cellular network. [96]

While the SQM has been used as the primary photometer in many light pollution studies, it remains a single-channel device with a relatively wide beam (20° FWHM; "SQM-L" version) that yields little information about the angular distribution of skyglow. The same is true of similar devices such as the Telescope Encoder and Sky Sensor-WiFi (TESS-W), introduced in 2017. [97] TESS-W was designed substantially like the SQM but uses a dichroic blocking filter to achieve better response at long wavelengths in order to detect skyglow contributions from sodium vapor lighting to wavelengths of nearly 800 nm. TESS-W has been cross-calibrated against the SQM to enable direct comparison between the two sources, which also defined an absolute astronomical photometric system for the device. [98]

One way of overcoming the poor angular resolution and limited interpretation utility of devices like the SQM and TESS-W is to interpolate gridded, point measurements of the night sky to generate crude all-sky maps. [99] However, these maps are surpassed in quality by wide-field or all-sky images made with multichannel radiance detectors. These data fall largely into two groups: those made with high-quality, low-noise 'astronomical' detectors, and those made with noisier consumer-grade detectors. The former tend to use charge-coupled devices (CCDs), while the latter tend to use active-pixel sensors based on complementary metal-oxide-semiconductor (CMOS) technology.

The most accurate measurements of the brightness of the night sky are those made with astronomical CCDs using telescopes as light collectors. Such measurements have high signal-to-noise (S/N) ratio and are often calibrated in absolute radiance units against spectrophotometric "standard stars". Sky brightness measurement programs have been undertaken at a number of astronomical observatories in order to better understand the nature of the natural night sky's influence on astronomical observations [100] monitor the impacts of artificial skyglow for the benefit of long-term site protection, [101] and determine the timescales and amplitudes of variability of natural light present in the night sky. [102,103] While astronomical measurements are highly reliable, they do not properly describe all-sky conditions due to the extremely small fields of view of most telescopes. In the sense of their utility in overall site characterization, they are

more like the family of single-channel detectors that provide no information about the full hemisphere of the night sky. They are also referred to particular passbands of astrophysical interest, which may not match the visual response of the human eye especially well.

Spectrophotometrically calibrated sky brightness measurements have also been successfully obtained with systems consisting of sensitive CCD detectors and wide-angle camera lenses. For example, the U.S. National Park Service (NPS) has built and extensively tested such a system, [104] which uses a camera and lens combination fixed to a motorized, programmable telescope mount. Over the course of about two hours, the camera captures images of the night sky on a series of grid points distributed in altitude and azimuth, slowly building up a mosaic view consisting of individual images that are later stitched together in software, corrected for pointing errors and projected as standard Hammer-Aitoff equal area maps (Figure 4). NPS has used the results to monitor the influence of light pollution on public lands in the United States. [105]

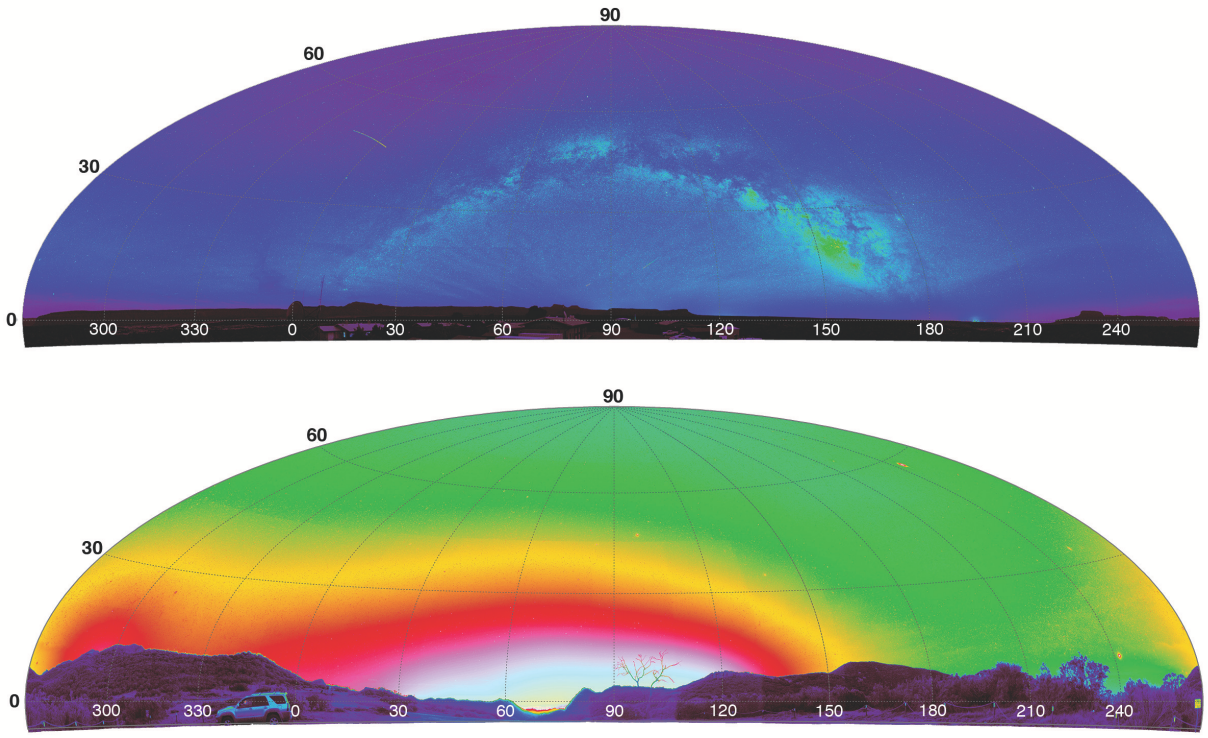

Figure 4. Examples of Hammer-Aitoff equal area all-sky maps of night sky brightness made in two locations using the National Park Service method illustrating the all-sky nighttime light distributions of both very naturally dark and heavily light polluted U.S. public lands. False colors indicate sky brightness in visual magnitudes per square arcsecond, ranging from +22 (purple) to +14 (white); warmer colors generally indicate brighter night skies. The locations are: Natural Bridges National Monument in Utah, U.S., 22 May 2012 (top) and Santa Monica Mountains National Recreation Area - Yerba Buena Trail in California, U.S., 17 February 2015 (bottom). Azimuth in degrees is indicated by the white labels, and altitude in degrees by the black labels. The Milky Way is evident from Natural Bridges, but is completely washed out in the Santa Monica Mountains due to light pollution from the greater Los Angeles metro area.

Although the results of the NPS method are very accurate, this approach has several drawbacks. The system is expensive and consists of bulky equipment that is not suitable for unattended operation

in the field. Operating the system requires specialist training to set up and collect images, as well as to reduce the data and produce the resulting maps. In order to increase the utility of the all-sky method of sky brightness characterization, and especially in the interest of making these imaging systems into long-term monitors, would require a method that is inexpensive, simple to operate, and autonomously operable.

An increasingly common approach along these lines is to use either an astronomical CCD or a consumer-grade CMOS sensor with an ultra-wide-angle lens such as a circular fisheye. An example of the former that has achieved some success is the All-Sky Transmission Monitor (ASTMON), [106] an autonomous, CCD-based continuous monitor of the surface brightness of the complete night sky in the Johnson-Cousins *UBVRI* photometric bands. [107] ASTMON is providing site monitoring in several places in Europe; a recent example of its use is to evaluate the impacts of lighting interventions in a nearby city on a protected site in Catalonia, Spain. [108] Similar systems have been tried using fewer broad passbands [109] and in narrow passbands using interference filters. [110]

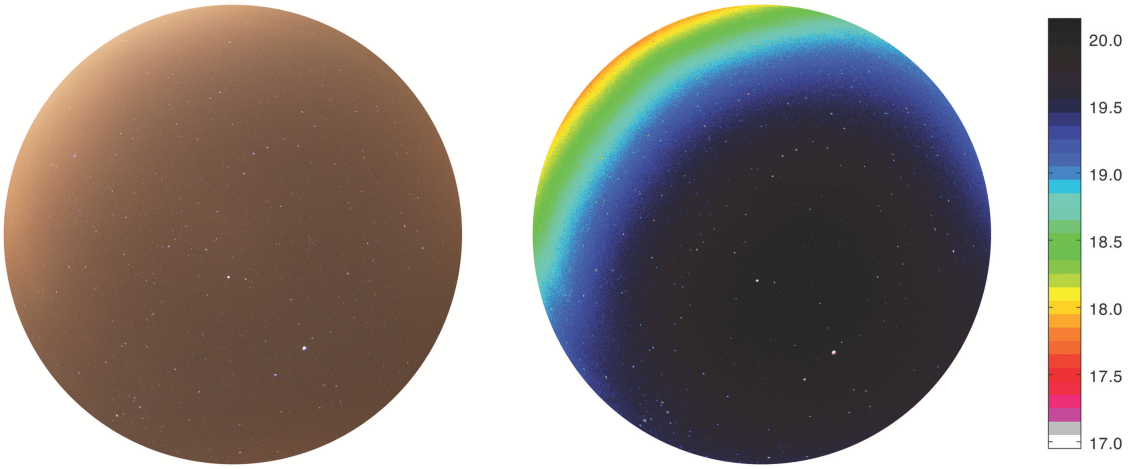

Figure 5. Uncalibrated (left) and luminance-calibrated (right) all-sky imagery of the night sky as seen from Mission San Xavier del Bac, 14 km south-southwest of the city center of Tucson, Arizona, U.S., on the night of UT 23 May 2017. The data were obtained using a Canon T5i DSLR body and a Sigma 4 mm circular fisheye lens, giving an apparent field of view of 180°. The images are positioned such that the zenith is at the center and the horizon at the edge of each, and they are oriented according to the usual astronomical convention of north at top and east at left. The warm tones in the uncalibrated image are indicative of the true color of skyglow near Tucson, whose city emissions are dominated by emissions from high-pressure sodium lighting. The false colors in the calibrated image correspond to luminances in units of visual magnitudes per square arcsecond according to the color bar at right.

These systems offer reliable operation in the field and a system of broad photometric passbands, but they are relatively expensive. A step down in photometric precision comes at a substantially reduced price and true portability; this approach involves off-the-shelf digital SLR (DSLR) camera bodies and fisheye lenses (Figure 5). These combinations are generally the least expensive of the all-sky monitoring options that can still produce reasonably precise photometry if referenced to calibrated light sources in the lab. They require little training to operate, and make use of both commercial [111] and freely distributed image reduction software. [112–114] Furthermore, their high portability enables night sky brightness measurements to be made in a variety of places, and even from moving platforms such as automobiles [115] and boats. [116] Time-series analysis of all-sky camera images can reveal considerably more information about the behavior of skyglow during, for example, light dimming tests than single-channel detectors measuring only fiducial sky locations like the zenith. [117]

These simple DLSR and fisheye lens combinations also suffer from certain limitations. Low angular resolution makes accurate stellar photometry difficult or impossible given that the stellar point spread function is severely undersampled; absent field calibration using spectrophotometric calibrators, the results are tied to lab calibration that may drift over time without periodic recalibration. And although most data reduction routines attempt to correct extreme angular distortion at the edges of the field, this introduces large photometric errors at the largest zenith angles.

Deriving spectral information from sky quality measurements adds an additional dimension to the existing axes of intensity and time. Spectroscopic observations with astronomical telescopes are the usual route to obtaining these data, but they generally sample only a very small part of the night sky and require relatively long exposure times to achieve high S/N. Nevertheless, this approach has been used to provide key information about the spectral power distributions of light emissions from cities whose skyglow threatens night sky quality over the sites of astronomical observatories. [118] Night sky spectra obtained over time allows observatories to monitor conditions and anticipate emerging threats. [119–122] Some limited spectral information about skyglow can be realized even for devices without an explicitly spectroscopic design mode. Kyba *et al.*, for instance, looked at differences in the RGB channels of output from commercial DSLR cameras, finding that the color of the night sky over cities varies according to the extent of local cloud cover. [123]

New directions in hyperspectral time-series imagery are already helping determine lighting usage in cities using a kind of ground-based 'remote sensing'. For example, Dobler *et al.* recently reported making high-cadence, time-series hyperspectral observations of the skyline of New York City, U.S., to generate a catalog of about 40 different urban lighting types. [124] Meanwhile, Alamús *et al.* used a similar hyperspectral imager to measure the spectral radiance of the urban nightscape in Barcelona, Catalonia, Spain, and to derive some useful photometric parameters from city scenes such as the photopic luminous efficacy of radiation (LER). [125]

A variety of analysis techniques have been developed to interpret spot measurements of broadband night sky brightness and time series observations in monitoring campaigns. One basic approach to visualizing a time series is to make representations such as so-called 'hourglass' or 'jellyfish' diagrams (Figure 6) that aggregate many nights' worth of sky brightness data into plots that code the frequencies of measurements according to a false-color scale. [126] Recently, Duriscoe showed that useful night sky quality metrics can be extracted from NPS maps of sky brightness, finding that the all-sky average brightness of the sky has the greatest utility in terms of characterizing the impact of skyglow on the nighttime environment, and that in this sense it outperforms the brightness of the night sky at the zenith. [105] Studies of the distribution of skyglow over ground sources have yielded procedures to retrieve the city emission function (CEF) with DSLR imagery. Kocifaj *et al.* recently showed how "inexpensive devices can properly identify the upward emissions with adequate reliability." [127]

Lastly, it is worth commenting on the ability of the human eye and brain to make meaningful estimates of the brightness of the night sky, which have clear utility in helping to characterize and monitor sites with respect to skyglow. Amateur astronomers have devised qualitative scales describing the quality of the night sky, [128] but coordinated citizen-science programs such as Globe At Night have yielded quantitative, scientifically useful measurements. [129,130] No equipment is needed to make the observations, and only minimal instruction is required to train observers; however, visual estimations of night sky brightness are ultimately subjective, impressionistic, and prone to variations among individual observers. Despite these drawbacks, programs like Globe At Night are clearly useful for drawing public attention to light pollution. [131]

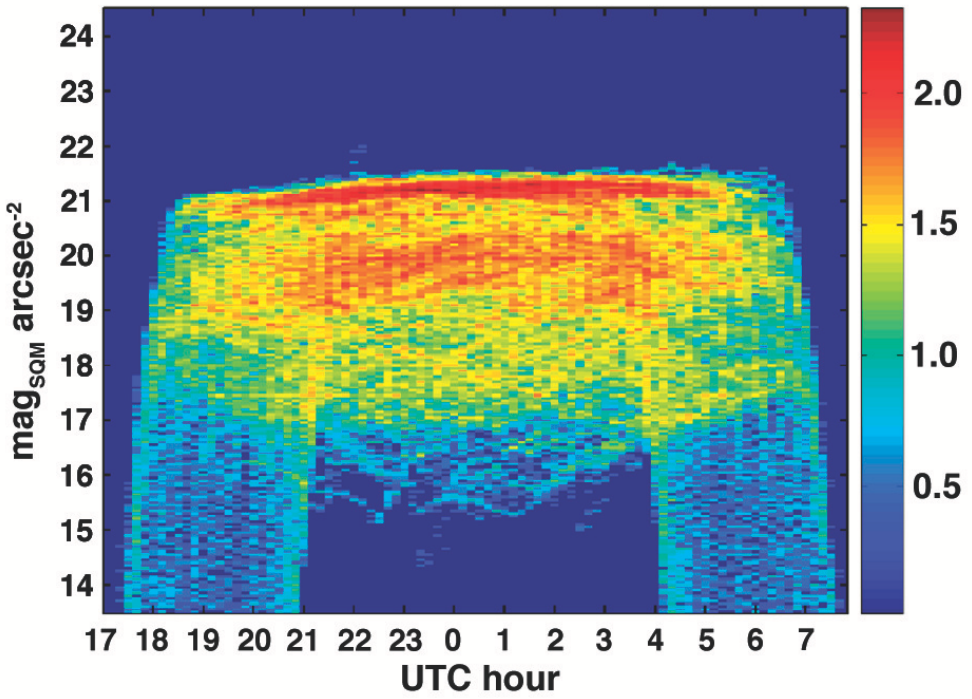

Figure 6. A night sky brightness densitogram, also known as a "jellyfish" plot. It shows the frequency with which particular values of the night sky brightness were recorded during the year 2018 in Paramos, Galicia, Spain. UTC time is shown on the abscissa in bins with a time resolution of 10 minutes, and sky luminance in magnitudes per square arcsecond (mpsa) on the ordinate in 0.05 mpsa bins. The colors indicate the frequency of measurements in the respective bins on a $\log_{10}$ scale. Adapted from Figure 1 from [95].

3. Modeling Skyglow

Models for the formation of skyglow are based on basic principles of radiative transfer applied to increasingly realistic scenarios in terms of light distribution on the ground and atmospheric conditions above. The earliest, phenomenological models were based on simple observations of skyglow at increasing distances from cities, augmented by low-resolution remote sensing data obtained from Earth orbit. In 1973 Walker established a simple empirical law relating the brightness of the night sky at the zenith seen from a particular distance from a city, finding that it scales exponentially with the city's population. [132,133] The same year Treanor published a relation for the brightness of the night sky at the zenith due to light pollution from a distant city, assuming the city was a point source of constant intensity and that ALAN propagated from source to observer via Mie scattering from aerosols in a plane-parallel atmosphere. [134] Later, modeling natural sources of light in the night sky, Staude added a spherical atmosphere treatment and the effects of first-order Rayleigh scattering. [135]

In the second half of the 1980s, Garstang devised a one-dimensional, self-consistent skyglow model from fundamental radiative transfer theory based on a two-dimensional source city with a uniform spatial distribution of light sources. [136,137] Realistic radiative transfer models of the time were severely limited by computational power, leading to generally crude results and many simplifying assumptions. Garstang's improved approach enabled fast computation of models by reducing the nature of the calculations to ray-tracing. But for nearly two decades, skyglow modeling was largely limited to clear atmospheres and a two-scattering approximation.

As processor cycles decreased in relative cost, skyglow models grew increasingly intricate. In the mid-2000s, new codes became available that began treating the complication of multiple-order scattering, [138] and which were later extended to consider the effects of ground reflection and topographic screening [139] as well as polarization of source rays during scattering events. [140] The characterization of atmospheric parameters became increasingly sophisticated as well, along with the ability to realistically simulate skyglow in cloudy to overcast conditions. [141] Cinzano and Falchi introduced what they called "extended Garstang models" that accounted for complications such as differences in site and source elevation; complex atmospheric situations such as thermal inversions; up to five aerosol layers in the upper atmosphere, and wavelength-dependent bidirectional ground reflectance. [142,143]

Kocifaj considered microphysical parameters of atmospheric aerosols in the scattering interactions that influence skyglow, devising a 'two-stream' approach and finding that the diffuse illuminance of the ground shows a local minimum at a particular value of the aerosol optical depth that does not depend on the size distribution of aerosols. [144] Recently, Kocifaj considered spectral ground albedo in a multiple-order scattering model, showing that the resulting night sky brightness has both an angular dependence and higher amplitudes at shorter wavelengths. [145]

Theorists have also developed mathematical and physical approaches to deal with the inverse problem, which is to retrieve the emission function of the light source from skyglow observations. This effort was pioneered by Kocifaj, who extensively investigated the influence of the city emission function on the resulting angular and intensity distribution of skyglow (Figure 7). [146–149] Importantly, in the course of this work Kocifaj found that the single-scattering approximation is "satisfactorily accurate" in modeling the distribution of light near the ground in cities because rays emitted or reflected upward into the night sky tend to scatter along relatively short paths, effectively 'trapping' many photons within the city environment. [150]

Other work has studied additional concerns beyond irradiance and/or illuminance distributions produced by skyglow, considering for example the spectral power distribution of sources as it tends to impact the visibility of skyglow at increasing distances from the source. Luginbuhl, Boley and Davis found that radiative transfer effects on skyglow formation depend strongly on the spectral power distribution

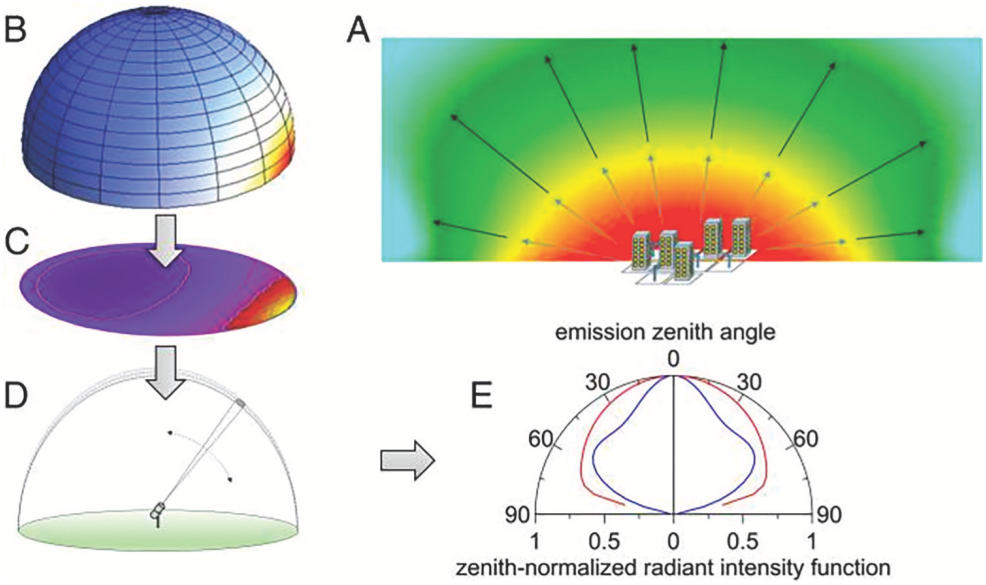

Figure 7. Retrieving the city emission function (CEF) from radiometry of the night sky. Light escaping from a city (A) propagates in all directions, but its distribution in 3-D space is complicated by various natural and artificial influences in the local environment including the distribution of light sources, wavelength-dependent surface albedos, and atmospheric conditions. Some of the photons are scattered back to the ground, and the resulting skyglow is seen over the hemisphere of sky (B) from an observation point outside the city. All-sky imaging techniques in clear-sky conditions record the distribution of light in the night sky (C), which can then be analyzed as a function of angular distance to the light source (D). Observations are inverted to yield the CEF. Two examples of the CEF are shown in (E). Figure 4 from [149].

of the source, particularly if the observation site is at a relatively large distance from the source. [12] This implies that blue-rich sources like white LED yield effectively more skyglow as perceived by the scotopically adapted human eye than sources with fewer blue emissions when seen at distances of several hundred kilometers.

Finally, a holistic view of the idea of 'modeling' light pollution should also consider how models inform understanding of the brightness of the natural night sky in the absence of anthropogenic light. Important work in this realm was done by the U.S. National Park Service in applying models of natural night sky phenomena to its all-sky mapping efforts. Duriscoe reported a technique by which the natural light contribution to night sky brightness is decomposed into multiple components representing sources such as (time-independent) airglow, the Milky Way, zodiacal light, and atmospheric diffuse light. [151] Models for each source are subtracted from all-sky imagery, leaving behind only the anthropogenic component. When applied in a conservation setting, this method can help practitioners better identify sources of light in the vicinity of a protected place in order to better guide efforts to mitigate their effects.

4. Needs: Measurements, Models, and Beyond

While many advancements in measuring and modeling ALAN were realized over the past several decades, data and research gaps continue to exist. While we propose a set of needs based upon our experience, there are no doubt many other needs that have already been or will be identified by the growing group of researchers seeking to better understand ALAN and the impacts it has on the environment and wellbeing of living things, including humans. Although research has already been carried out to a limited degree in some of these recognized areas, additional efforts are still needed even where inroads have been made.

4.1. Measurements

Many measurements of light pollution now exist in the literature, both radiometric and photometric in nature, and obtained from the ground to outer space. However, there is no standardized system of metrology for ALAN traceable to the SI system of units, which has resulted in the use of a wide variety of methods, instruments and metrics. Lack of a standardized system makes the intercomparison of most existing light pollution measurements difficult, if not impossible. We, therefore, argue in favor of standardization in order to promote more purposeful interpretation of ALAN data. A new system of ALAN metrology entails the development of standard calibration methods that will in turn lead to more reliable measurement replication, especially for lower-cost equipment that is more readily utilized in the field.

We also recognize the useful limit of information about skyglow that can be provided by single-channel photometers such as the Sky Quality Meter. A holistic approach to characterizing the brightness of the night sky yields information about the angular distribution of light with sufficient resolution to identify ground-based sources, which inevitably involves some form of two-dimensional imaging. There is now a clear need for portable, autonomous, reliable, low-cost, field-robust imaging systems for both initial site characterization and long-term monitoring. These systems should have panchromatic responses to light across the optical spectrum, and for the benefit of measuring impacts to wildlife affected by ALAN sensitive to those wavelengths, extended response in the near-ultraviolet and near-infrared. Development of new hardware, and perhaps emerging methods such as hyperspectral imagery, are needed.

Remote sensing of ALAN is in need of wider spectral response and better spatial resolution, especially among satellite-based facilities. At present the best available platform with global coverage and nightly cadence, VIIRS-DNB, is effectively blind to a significant fraction of the total spectral power emitted by modern outdoor lighting equipment. Additionally, satellite observations of night lights are almost always incidental to primary missions, which are typically based on meteorology or daytime earth observation.

We argue that the time has come for a dedicated satellite mission to sense ALAN whose parameters are responsive to science drivers. These drivers include (but are not limited to) investigation of ALAN as it penetrates into more complicated environments such as into water bodies and forested areas, and within urban spaces; measuring and monitoring particular lighting applications such as oil and natural gas extraction, mining, global shipping and fishing; and determining the contribution of ALAN to energy budgets within ecological systems.

Scientific investigations may be carried out through multiple modes of investigation, potentially coordinated between remote sensing with high-altitude measurements from satellites, mid-altitude measurements from airplanes and/or weather balloons, low-altitude measurements from airplanes and/or drones, and ground-level measurements from stationary monitoring stations and moving platforms. Coordinated investigations offer for new opportunities for research, including tracking of mobile sources of ALAN; ALAN coverage of ecological landscapes; and continued exploration of expected natural variations in the brightness of the night sky, absent ALAN, through the solar and lunar cycles. Our ability to determine variability of natural night sky brightness will be important as we also begin to focus on exposure assessments for ALAN needed for ecological health and human health studies. Methods for measuring light dosage, light exposure, and sensory response and receptor response to light are critical to assessing the biological impact of ALAN.

4.2. Modeling

Difficult computational problems become progressively easier to solve as the cost and time of computer processor cycles continues to fall. Radiative transfer models of ALAN propagation and skyglow will become progressively more sophisticated, incorporating increasingly realistic physics. New models will bring favorable circumstances to explore new areas of research, including evaluating the impact of LED chromaticity shift on skyglow, exploring the impact of ground cover (snow, wet conditions, vegetation) on ALAN propagation, assessing factors controlling variability of night sky brightness, and determining the minimum set of parameters needed to model urban light emissions so as to be able to accurately retrieve the city emission function.

Like measurement techniques, models of both sky brightness and ground light distributions seen from space will also benefit from improved angular and spatial resolution. Additionally, there is a need to better link the upwelling radiance from a given location as seen from space to the luminance of the night sky as seen from the ground. Solving this problem will allow satellite observations to become progressively better at predicting the quality of the night sky as seen from places where no ground measurements are available and tracking night sky quality and its evolution over time in particular locations.

An ability to render ALAN across landscapes using geographic information system (GIS)-based mapping will help solve modeling problems associated with ALAN propagation due to landscape elevation and ground cover. Future ALAN models should also characterize the distribution and propagation of light at wavelengths outside of the visible spectrum to which wildlife are acutely sensitive. Visualizations should consider not only the perception of the human eye, but also that of other species including birds, mammals, reptiles, amphibians and insects that view the world in ways often rather different from humans. Developed models used to assess and track propagation and exposure to ALAN from the perspective of upward radiance and ground level illuminance mapping systems are needed to aid in policy formation, provide guidance to lighting designers, predict how ALAN will change over time, and to perform ALAN exposure and health assessments.

4.3. Beyond Data and Models

The observation, quantitative measurement, and modeling of ALAN work together in increasingly complex ways to suggest new avenues of research in this field. There are still a number of open questions that these tools can help answer, including the following.

What is "darkness"? The meaning of this question is different in varied contexts: astronomical, ecological, and social. The most visible manifestation of nighttime darkness – the night sky – is similarly affected: what is a "dark sky"? This adds a distinct aesthetic dimension to the measurement and modeling of light and dark, and determining systematically the proper quantity of light for safe task performance and other outdoor applications. The recognized standards organizations that publish lighting recommendations for various applications now do so largely by achieving the consensus of practitioners of lighting design and engineering based on their professional experience rather than on any rigorous empirical evidence. [152] Effectively managing the use of ALAN such that legitimate human needs are met while protecting to the greatest practical extent the integrity of natural darkness depends crucially on addressing this question.

How can measurements and models best inform resource conservation? As natural nighttime darkness emerges as a global conservation value, it may be useful to take a cue from that field and examine which factors influence the preservation, conservation, and restoration of the natural night sky resource. As sources of water and unimpeded natural views are denoted by the terms "watersheds" and "viewsheds," respectively, we may consider geographic "skysheds" as covering ecological landscapes that are likely to be more sensitive to ALAN impacts. Rigorously defining these regions geographically and topographically will aid in determining threshold light exposure levels targeted to particular ecological protections.

While most of the needs identified here are practical in nature, several also should be considered theoretical and or philosophical. While we have done our best to group the needs based upon measurements, models, and beyond, we realize that most needs cross transdisciplinary boundaries and knowledge bases. Therefore, as these needs are realized (and other needs emerge) we hope that the Journal of Dark Sky Studies will serve as a viable community of researchers representing contributions to measurements and modeling of ALAN from across disciplines.

Author Contributions: All authors contributed equally to the preparation of this manuscript.

Funding: This research received no external funding.

Acknowledgments: The authors thank the following individuals for granting permission to reproduce various figures in this paper: Ken Walczak and Geza Gyuk (Figure 3); Salva Bará, Raul Lima and Jaime Zamorano (Figure 6); and Miroslav Kocifaj, Héctor Solano-Lamphar and Gorden Videen (Figure 7).

This paper is dedicated to the memory of Thomas Posch (1974–2019), whose contributions to light pollution research endure.

Conflicts of Interest: The authors declare no conflict of interest.

References

1. Wurtman, R.J. The Pineal and Endocrine Function. *Hospital Practice* **1969**, *4*, 32–37. doi:10.1080/21548331.1969.11704296.
2. Sperling, N. The Disappearance of Darkness. IAU Colloq. 112: Light Pollution, Radio Interference, and Space Debris; Crawford, D.L., Ed., 1991, Vol. 17, *Astronomical Society of the Pacific Conference Series*, p. 101.
3. Brox, J. Out of the Dark: A Brief History of Artificial Light in Outdoor Spaces. In *Urban Lighting, Light Pollution and Society*, 1st ed.; Meier, J.; Hasenōhrl, U.; Krause, K.; Pottharst, M., Eds.; Routledge, 2015; chapter 1, pp. 13–29.
4. Dutcher, W. Bird Notes from Long Island, N. Y. *The Auk* **1885**, *2*, 36–39. doi:10.2307/4625170.

5. Thompson, G. Spiders and the Electric Light. *Science* **1887**, *9*, 92.
6. Hamilton, J. Electric Light Captures. *Psyche: A Journal of Entomology* **1889**, *5*, 149–150. doi:10.1155/1889/20196.
7. Falchi, F.; Cinzano, P.; Duriscoe, D.; Kyba, C.; Elvidge, C.; Baugh, K.; Portnov, B.; Rybnikova, N.; Furgoni, R. The new world atlas of artificial night sky brightness. *Science Advances* **2016**, *2*. doi:10.1126/sciadv.1600377.
8. Kyba, C.C.M.; Kuester, T.; Sánchez de Miguel, A.; Baugh, K.; Jechow, A.; Hölker, F.; Bennie, J.; Elvidge, C.D.; Gaston, K.J.; Guanter, L. Artificially lit surface of Earth at night increasing in radiance and extent. *Science Advances* **2017**, *3*. doi:10.1126/sciadv.1701528.
9. Falchi, F.; Furgoni, R.; Gallaway, T.; Rybnikova, N.; Portnov, B.; Baugh, K.; Cinzano, P.; Elvidge, C. Light pollution in USA and Europe: The good, the bad and the ugly. *Journal of Environmental Management* **2019**, *248*, 109227. doi:10.1016/j.jenvman.2019.06.128.
10. Falchi, F.; Cinzano, P.; Elvidge, C.D.; Keith, D.M.; Haim, A. Limiting the impact of light pollution on human health, environment and stellar visibility. *Journal of Environmental Management* **2011**, *92*, 2714–2722. doi:10.1016/j.jenvman.2011.06.029.
11. Aubé, M.; Roby, J.; Kocifaj, M. Evaluating Potential Spectral Impacts of Various Artificial Lights on Melatonin Suppression, Photosynthesis, and Star Visibility. *PLoS ONE* **2013**, *8*, e67798. doi:10.1371/journal.pone.0067798.
12. Luginbuhl, C.B.; Boley, P.A.; Davis, D.R. The impact of light source spectral power distribution on sky glow. *Journal of Quantitative Spectroscopy and Radiative Transfer* **2014**, *139*, 21–26. doi:10.1016/j.jqsrt.2013.12.004.
13. La Sorte, F.A.; Fink, D.; Buler, J.J.; Farnsworth, A.; Cabrera-Cruz, S.A. Seasonal associations with urban light pollution for nocturnally migrating bird populations. *Global Change Biology* **2017**, *23*, 4609–4619. doi:10.1111/gcb.13792.
14. Rodríguez, A.; Holmes, N.D.; Ryan, P.G.; Wilson, K.J.; Faulquier, L.; Murillo, Y.; Raine, A.F.; Penniman, J.F.; Neves, V.; Rodríguez, B.; Negro, J.J.; Chiaradia, A.; Dann, P.; Anderson, T.; Metzger, B.; Shirai, M.; Deppe, L.; Wheeler, J.; Hodum, P.; Gouveia, C.; Carmo, V.; Carreira, G.P.; Delgado-Alburqueque, L.; Guerra-Correa, C.; Couzi, F.X.; Travers, M.; Corre, M.L. Seabird mortality induced by land-based artificial lights. *Conservation Biology* **2017**, *31*, 986–1001. doi:10.1111/cobi.12900.
15. Doren, B.M.V.; Horton, K.G.; Dokter, A.M.; Klinck, H.; Elbin, S.B.; Farnsworth, A. High-intensity urban light installation dramatically alters nocturnal bird migration. *Proceedings of the National Academy of Sciences* **2017**, *114*, 11175–11180. doi:10.1073/pnas.1708574114.
16. de Jong, M.; van den Eertwegh, L.; Beskers, R.E.; de Vries, P.P.; Spoelstra, K.; Visser, M.E. Timing of Avian Breeding in an Urbanised World. *Ardea* **2018**, *106*, 31. doi:10.5253/arde.v106i1.a4.
17. Brüning, A.; Hölker, F.; Wolter, C. Artificial light at night: implications for early life stages development in four temperate freshwater fish species. *Aquatic Sciences* **2011**, *73*, 143–152. doi:10.1007/s00027-010-0167-2.
18. Becker, A.; Whitfield, A.K.; Cowley, P.D.; Järnegren, J.; Næsje, T.F. Potential effects of artificial light associated with anthropogenic infrastructure on the abundance and foraging behaviour of estuary-associated fishes. *Journal of Applied Ecology* **2013**, *50*, 43–50. doi:10.1111/1365-2664.12024.
19. Bengsen, A.J.; Leung, L.K.P.; Lapidge, S.J.; Gordon, I.J. Artificial illumination reduces bait-take by small rainforest mammals. *Applied Animal Behaviour Science* **2010**, *127*, 66–72. doi:https://doi.org/10.1016/j.applanim.2010.08.006.
20. Robert, K.A.; Lesku, J.A.; Partecke, J.; Chambers, B. Artificial light at night desynchronizes strictly seasonal reproduction in a wild mammal. *Proceedings of the Royal Society B: Biological Sciences* **2015**, *282*, 20151745. doi:10.1098/rspb.2015.1745.
21. Hoffmann, J.; Palme, R.; Eccard, J.A. Long-term dim light during nighttime changes activity patterns and space use in experimental small mammal populations. *Environmental Pollution* **2018**, *238*, 844–851. doi:https://doi.org/10.1016/j.envpol.2018.03.107.
22. Lorne, J.K.; Salmon, M. Effects of exposure to artificial lighting on orientation of hatchling sea turtles on the beach and in the ocean. *Endangered Species Research* **2007**, *3*, 23–30. doi:10.3354/esr003023.

23. Kamrowski, R.; Limpus, C.; Moloney, J.; Hamann, M. Coastal light pollution and marine turtles: assessing the magnitude of the problem. *Endangered Species Research* **2012**, *19*, 85–98. doi:10.3354/esr00462.
24. Zheleva, M. The dark side of light. Light pollution kills leatherback turtle hatchlings. *BioDiscovery* **2012**, *3*, e8930. doi:10.7750/BioDiscovery.2012.3.4.
25. Macgregor, C.J.; Evans, D.M.; Fox, R.; Pocock, M.J.O. The dark side of street lighting: impacts on moths and evidence for the disruption of nocturnal pollen transport. *Global Change Biology* **2017**, *23*, 697–707. doi:10.1111/gcb.13371.
26. Davies, T.W.; Bennie, J.; Cruse, D.; Blumgart, D.; Inger, R.; Gaston, K.J. Multiple night-time light-emitting diode lighting strategies impact grassland invertebrate assemblages. *Global Change Biology* **2017**, *23*, 2641–2648. doi:10.1111/gcb.13615.
27. Underwood, C.N.; Davies, T.W.; Queirós, A.M. Artificial light at night alters trophic interactions of intertidal invertebrates. *Journal of Animal Ecology* **2017**, *86*, 781–789. doi:10.1111/1365-2656.12670.
28. Bennie, J.; Davies, T.W.; Cruse, D.; Inger, R.; Gaston, K.J. Artificial light at night causes top-down and bottom-up trophic effects on invertebrate populations. *Journal of Applied Ecology* **2018**, *55*, 2698–2706. doi:10.1111/1365-2664.13240.
29. Bennie, J.; Davies, T.W.; Cruse, D.; Gaston, K.J. Ecological effects of artificial light at night on wild plants. *Journal of Ecology* **2016**, *104*, 611–620. doi:10.1111/1365-2745.12551.
30. Škvareninová, J.; Tuhárska, M.; Škvarenina, J.; Babálová, D.; Slobodníková, L.; Slobodník, B.; Středová, H.; Minďaš, J. Effects of light pollution on tree phenology in the urban environment. *Moravian Geographical Reports* **2017**, *25*, 282–290. doi:10.1515/mgr-2017-0024.
31. Brelsford, C.C.; Robson, T.M. Blue light advances bud burst in branches of three temperate deciduous tree species under short-day conditions. *Trees* **2018**, *32*, 1157–1164. doi:10.1007/s00468-018-1684-1.
32. Walmsley, L.; Hanna, L.; Mouland, J.; Martial, F.; West, A.; Smedley, A.R.; Bechtold, D.A.; Webb, A.R.; Lucas, R.J.; Brown, T.M. Colour As a Signal for Entraining the Mammalian Circadian Clock. *PLOS Biology* **2015**, *13*, e1002127. doi:10.1371/journal.pbio.1002127.
33. Lewy, A.; Wehr, T.; Goodwin, F.; Newsome, D.; Markey, S. Light suppresses melatonin secretion in humans. *Science* **1980**, *210*, 1267–1269. doi:10.1126/science.7434030.
34. Carrillo-Vico, A.; Guerrero, J.M.; Lardone, P.J.; Reiter, R.J. A Review of the Multiple Actions of Melatonin on the Immune System. *Endocrine* **2005**, *27*, 189–200. doi:10.1385/endo:27:2:189.
35. Zubidat, A.E.; Haim, A. Artificial light-at-night – a novel lifestyle risk factor for metabolic disorder and cancer morbidity. *Journal of Basic and Clinical Physiology and Pharmacology* **2017**, *28*. doi:10.1515/jbcpp-2016-0116.
36. Xie, Y.; Weng, Q.; Fu, P. Temporal variations of artificial nighttime lights and their implications for urbanization in the conterminous United States, 2013–2017. *Remote Sensing of Environment* **2019**, *225*, 160–174. doi:10.1016/j.rse.2019.03.008.
37. Wu, R.; Yang, D.; Dong, J.; Zhang, L.; Xia, F. Regional Inequality in China Based on NPP-VIIRS Night-Time Light Imagery. *Remote Sensing* **2018**, *10*, 240. doi:10.3390/rs10020240.
38. Chen, X.; Nordhaus, W.D. VIIRS Nighttime Lights in the Estimation of Cross-Sectional and Time-Series GDP. *Remote Sensing* **2019**, *11*, 1057. doi:10.3390/rs11091057.
39. Fehrer, D.; Krarti, M. Spatial distribution of building energy use in the United States through satellite imagery of the earth at night. *Building and Environment* **2018**, *142*, 252–264. doi:10.1016/j.buildenv.2018.06.033.
40. Jasiński, T. Modeling electricity consumption using nighttime light images and artificial neural networks. *Energy* **2019**, *179*, 831–842. doi:10.1016/j.energy.2019.04.221.
41. Falchetta, G.; Pachauri, S.; Parkinson, S.; Byers, E. A high-resolution gridded dataset to assess electrification in sub-Saharan Africa. *Scientific Data* **2019**, *6*. doi:10.1038/s41597-019-0122-6.
42. Levin, N.; Ali, S.; Crandall, D. Utilizing remote sensing and big data to quantify conflict intensity: The Arab Spring as a case study. *Applied Geography* **2018**, *94*, 1–17. doi:10.1016/j.apgeog.2018.03.001.
43. Levin, N.; Ali, S.; Crandall, D.; Kark, S. World Heritage in danger: Big data and remote sensing can help protect sites in conflict zones. *Global Environmental Change* **2019**, *55*, 97–104. doi:10.1016/j.gloenvcha.2019.02.001.

44. Li, X.; Liu, S.; Jendryke, M.; Li, D.; Wu, C. Night-Time Light Dynamics during the Iraqi Civil War. *Remote Sensing* **2018**, *10*, 858. doi:10.3390/rs10060858.
45. Zhao, X.; Yu, B.; Liu, Y.; Yao, S.; Lian, T.; Chen, L.; Yang, C.; Chen, Z.; Wu, J. NPP-VIIRS DNB Daily Data in Natural Disaster Assessment: Evidence from Selected Case Studies. *Remote Sensing* **2018**, *10*, 1526. doi:10.3390/rs10101526.
46. Román, M.O.; Stokes, E.C.; Shrestha, R.; Wang, Z.; Schultz, L.; Carlo, E.A.S.; Sun, Q.; Bell, J.; Molthan, A.; Kalb, V.; Ji, C.; Seto, K.C.; McClain, S.N.; Enenkel, M. Satellite-based assessment of electricity restoration efforts in Puerto Rico after Hurricane Maria. *PLOS ONE* **2019**, *14*, e0218883. doi:10.1371/journal.pone.0218883.
47. Heger, M.P.; Neumayer, E. The impact of the Indian Ocean tsunami on Aceh's long-term economic growth. *Journal of Development Economics* **2019**, *141*, 102365. doi:10.1016/j.jdeveco.2019.06.008.
48. Garcia-Saenz, A.; de Miguel, A.S.; Espinosa, A.; Valentin, A.; Aragonés, N.; Llorca, J.; Amiano, P.; Sánchez, V.M.; Guevara, M.; Capelo, R.; Tardón, A.; Peiró-Perez, R.; Jiménez-Moleón, J.J.; Roca-Barceló, A.; Pérez-Gómez, B.; Dierssen-Sotos, T.; Fernández-Villa, T.; Moreno-Iribas, C.; Moreno, V.; García-Pérez, J.; Castaño-Vinyals, G.; Pollán, M.; Aubé, M.; Kogevinas, M. Evaluating the Association between Artificial Light-at-Night Exposure and Breast and Prostate Cancer Risk in Spain (MCC-Spain Study). *Environmental Health Perspectives* **2018**, *126*, 047011. doi:10.1289/ehp1837.
49. Geronimo, R.; Franklin, E.; Brainard, R.; Elvidge, C.; Santos, M.; Venegas, R.; Mora, C. Mapping Fishing Activities and Suitable Fishing Grounds Using Nighttime Satellite Images and Maximum Entropy Modelling. *Remote Sensing* **2018**, *10*, 1604. doi:10.3390/rs10101604.
50. Ghosh, T.; Anderson, S.; Elvidge, C.; Sutton, P. Using Nighttime Satellite Imagery as a Proxy Measure of Human Well-Being. *Sustainability* **2013**, *5*, 4988–5019. doi:10.3390/su5124988.
51. Gillespie, T.W.; Willis, K.S.; Ostermann-Kelm, S.; Longcore, T.; Federico, F.; Lee, L.; MacDonald, G.M. Inventorying and Monitoring Nighttime Light Distribution and Dynamics in the Mediterranean Coast Network of Southern California. *Natural Areas Journal* **2017**, *37*, 350–360. doi:10.3375/043.037.0309.
52. Guetté, A.; Godet, L.; Juigner, M.; Robin, M. Worldwide increase in Artificial Light At Night around protected areas and within biodiversity hotspots. *Biological Conservation* **2018**, *223*, 97–103. doi:https://doi.org/10.1016/j.biocon.2018.04.018.
53. Xu, P.; Wang, Q.; Jin, J.; Jin, P. An increase in nighttime light detected for protected areas in mainland China based on VIIRS DNB data. *Ecological Indicators* **2019**, *107*, 105615. doi:10.1016/j.ecolind.2019.105615.
54. Hyde, E.; Frank, S.; Barentine, J.C.; Kuechly, H.; Kyba, C.C.M. Testing for changes in light emissions from certified International Dark Sky Places. *International Journal of Sustainable Lighting* **2019**, *21*, 11–19. doi:10.26607/ijsl.v21i1.92.
55. Stark, H.; Brown, S.S.; Wong, K.W.; Stutz, J.; Elvidge, C.D.; Pollack, I.B.; Ryerson, T.B.; Dube, W.P.; Wagner, N.L.; Parrish, D.D. City lights and urban air. *Nature Geoscience* **2011**, *4*, 730–731. doi:10.1038/ngeo1300.
56. Fu, D.; Xia, X.; Duan, M.; Zhang, X.; Li, X.; Wang, J.; Liu, J. Mapping nighttime PM2.5 from VIIRS DNB using a linear mixed-effect model. *Atmospheric Environment* **2018**, *178*, 214–222. doi:10.1016/j.atmosenv.2018.02.001.
57. Zhang, J.; Jaker, S.L.; Reid, J.S.; Miller, S.D.; Solbrig, J.; Toth, T.D. Characterization and application of artificial light sources for nighttime aerosol optical depth retrievals using the Visible Infrared Imager Radiometer Suite Day/Night Band. *Atmospheric Measurement Techniques* **2019**, *12*, 3209–3222. doi:10.5194/amt-12-3209-2019.
58. Doll, C.H.; Muller, J.P.; Elvidge, C.D. Night-time Imagery as a Tool for Global Mapping of Socioeconomic Parameters and Greenhouse Gas Emissions. *AMBIO: A Journal of the Human Environment* **2000**, *29*, 157–162. doi:10.1579/0044-7447-29.3.157.
59. Elvidge, C.D.; Erwin, E.H.; Baugh, K.E.; Ziskin, D.; Tuttle, B.T.; Ghosh, T.; Sutton, P.C. Overview of DMSP nightime lights and future possibilities. 2009 Joint Urban Remote Sensing Event. IEEE, 2009. doi:10.1109/urs.2009.5137749.
60. Cinzano, P.; Falchi, F.; Elvidge, C. The first World Atlas of the artificial night sky brightness. *Monthly Notices of the Royal Astronomical Society* **2001**, *328*, 689–707. doi:10.1046/j.1365-8711.2001.04882.x.
61. Elvidge, C.D.; Baugh, K.E.; Zhizhin, M.; Hsu, F.C. Why VIIRS data are superior to DMSP for mapping nighttime lights. *Proceedings of the Asia-Pacific Advanced Network* **2013**, *35*, 62. doi:10.7125/apan.35.7.

62. Huang, Q.; Yang, X.; Gao, B.; Yang, Y.; Zhao, Y. Application of DMSP/OLS Nighttime Light Images: A Meta-Analysis and a Systematic Literature Review. *Remote Sensing* **2014**, *6*, 6844–6866. doi:10.3390/rs6086844.
63. Cao, X.; Hu, Y.; Zhu, X.; Shi, F.; Zhuo, L.; Chen, J. A simple self-adjusting model for correcting the blooming effects in DMSP-OLS nighttime light images. *Remote Sensing of Environment* **2019**, *224*, 401–411. doi:https://doi.org/10.1016/j.rse.2019.02.019.
64. Cao, C.; Luccia, F.J.D.; Xiong, X.; Wolfe, R.; Weng, F. Early On-Orbit Performance of the Visible Infrared Imaging Radiometer Suite Onboard the Suomi National Polar-Orbiting Partnership (S-NPP) Satellite. *IEEE Transactions on Geoscience and Remote Sensing* **2014**, *52*, 1142–1156. doi:10.1109/tgrs.2013.2247768.
65. Kyba, C.; Garz, S.; Kuechly, H.; de Miguel, A.; Zamorano, J.; Fischer, J.; Hölker, F. High-Resolution Imagery of Earth at Night: New Sources, Opportunities and Challenges. *Remote Sensing* **2014**, *7*, 1–23. doi:10.3390/rs70100001.
66. Lee, T.E.; Miller, S.D.; Turk, F.J.; Schueler, C.; Julian, R.; Deyo, S.; Dills, P.; Wang, S. The NPOESS VIIRS Day/Night Visible Sensor. *Bulletin of the American Meteorological Society* **2006**, *87*, 191–200. doi:10.1175/bams-87-2-191.
67. Liao, L.B.; Weiss, S.; Mills, S.; Hauss, B. Suomi NPP VIIRS day-night band on-orbit performance. *Journal of Geophysical Research: Atmospheres* **2013**, *118*, 12705–12718. doi:10.1002/2013JD020475.
68. Coesfeld, J.; Anderson, S.; Baugh, K.; Elvidge, C.; Schernthanner, H.; Kyba, C. Variation of Individual Location Radiance in VIIRS DNB Monthly Composite Images. *Remote Sensing* **2018**, *10*, 1964. doi:10.3390/rs10121964.
69. Duriscoe, D.M.; Anderson, S.J.; Luginbuhl, C.B.; Baugh, K.E. A simplified model of all-sky artificial sky glow derived from VIIRS Day/Night band data. *Journal of Quantitative Spectroscopy and Radiative Transfer* **2018**, *214*, 133–145. doi:https://doi.org/10.1016/j.jqsrt.2018.04.028.
70. Zheng, Q.; Weng, Q.; Wang, K. Developing a new cross-sensor calibration model for DMSP-OLS and Suomi-NPP VIIRS night-light imageries. *ISPRS Journal of Photogrammetry and Remote Sensing* **2019**, *153*, 36–47. doi:10.1016/j.isprsjprs.2019.04.019.
71. Bará, S.; Rigueiro, I.; Lima, R.C. Monitoring transition: Expected night sky brightness trends in different photometric bands. *Journal of Quantitative Spectroscopy and Radiative Transfer* **2019**, *239*, 106644. doi:10.1016/j.jqsrt.2019.106644.
72. Levin, N.; Johansen, K.; Hacker, J.M.; Phinn, S. A new source for high spatial resolution night time images — The EROS-B commercial satellite. *Remote Sensing of Environment* **2014**, *149*, 1–12. doi:10.1016/j.rse.2014.03.019.
73. Zhang, G.; Li, L.; Jiang, Y.; Shen, X.; Li, D. On-Orbit Relative Radiometric Calibration of the Night-Time Sensor of the LuoJia1-01 Satellite. *Sensors* **2018**, *18*, 4225. doi:10.3390/s18124225.
74. Jiang, W.; He, G.; Long, T.; Guo, H.; Yin, R.; Leng, W.; Liu, H.; Wang, G. Potentiality of Using Luojia 1-01 Nighttime Light Imagery to Investigate Artificial Light Pollution. *Sensors* **2018**, *18*, 2900. doi:10.3390/s18092900.
75. Zhang, G.; Wang, J.; Jiang, Y.; Zhou, P.; Zhao, Y.; Xu, Y. On-Orbit Geometric Calibration and Validation of Luojia 1-01 Night-Light Satellite. *Remote Sensing* **2019**, *11*, 264. doi:10.3390/rs11030264.
76. Li, X.; Li, X.; Li, D.; He, X.; Jendryke, M. A preliminary investigation of Luojia-1 night-time light imagery. *Remote Sensing Letters* **2019**, *10*, 526–535. doi:10.1080/2150704x.2019.1577573.
77. Zheng, Q.; Weng, Q.; Huang, L.; Wang, K.; Deng, J.; Jiang, R.; Ye, Z.; Gan, M. A new source of multi-spectral high spatial resolution night-time light imagery—JL1-3B. *Remote Sensing of Environment* **2018**, *215*, 300–312. doi:https://doi.org/10.1016/j.rse.2018.06.016.
78. Elvidge, C.D.; Cinzano, P.; Pettit, D.R.; Arvesen, J.; Sutton, P.; Small, C.; Nemani, R.; Longcore, T.; Rich, C.; Safran, J.; Weeks, J.; Ebener, S. The Nightsat mission concept. *International Journal of Remote Sensing* **2007**, *28*, 2645–2670. doi:10.1080/01431160600981525.
79. Elvidge, C.D.; Keith, D.M.; Tuttle, B.T.; Baugh, K.E. Spectral Identification of Lighting Type and Character. *Sensors* **2010**, *10*, 3961–3988. doi:10.3390/s100403961.

80. Walczak, K.; Gyuk, G.; Kruger, A.; Byers, E.; Huerta, S. NITESat: A High Resolution, Full-Color, Light Pollution Imaging Satellite Mission. *International Journal of Sustainable Lighting* **2017**, *19*, 48–55. doi:10.26607/ijsl.v19i1.68.
81. Kyba, C.C.M.; Ruhtz, T.; Lindemann, C.; Fischer, J.; Hölker, F. Two camera system for measurement of urban uplight angular distribution. AIP, 2013. doi:10.1063/1.4804833.
82. Kuechly, H.U.; Kyba, C.C.; Ruhtz, T.; Lindemann, C.; Wolter, C.; Fischer, J.; Hölker, F. Aerial survey and spatial analysis of sources of light pollution in Berlin, Germany. *Remote Sensing of Environment* **2012**, *126*, 39–50. doi:10.1016/j.rse.2012.08.008.
83. Hale, J.D.; Davies, G.; Fairbrass, A.J.; Matthews, T.J.; Rogers, C.D.F.; Sadler, J.P. Mapping Lightscapes: Spatial Patterning of Artificial Lighting in an Urban Landscape. *PLoS ONE* **2013**, *8*, e61460. doi:10.1371/journal.pone.0061460.
84. Barentine, J.C. Methods for Assessment and Monitoring of Light Pollution around Ecologically Sensitive Sites. *Journal of Imaging* **2019**, *5*, 54. doi:10.3390/jimaging5050054.
85. Walczak, K.; Gyuk, G. NITELite: Balloon-borne Observations of Nighttime Lighting. Light Pollution: Theory Modeling and Measurements, Hajmás, Hungary, 25-28 June 2019, 2019.
86. Sánchez de Miguel, A.; Castano, J.G.; Zamorano, J.; Pascual, S.; Angeles, M.; Cayuela, L.; Martinez, G.M.; Challupner, P.; Kyba, C.C.M. Atlas of astronaut photos of Earth at night. *Astronomy & Geophysics* **2014**, *55*, 4.36–4.36. doi:10.1093/astrogeo/atu165.
87. Sánchez de Miguel, A. Variación Espacial, Temporal Y Espectral De La Contaminación Lumínica Y Sus Fuentes: Metodología Y Resultados. PhD thesis, Universidad Complutense de Madrid, 2015. doi:10.5281/zenodo.1422725.
88. Sánchez de Miguel, A.; Kyba, C.C.; Aubé, M.; Zamorano, J.; Cardiel, N.; Tapia, C.; Bennie, J.; Gaston, K.J. Colour remote sensing of the impact of artificial light at night (I): The potential of the International Space Station and other DSLR-based platforms. *Remote Sensing of Environment* **2019**, *224*, 92–103. doi:https://doi.org/10.1016/j.rse.2019.01.035.
89. Sánchez de Miguel, A.; Aubé, M.; Zamorano, J.; Kocifaj, M.; Roby, J.; Tapia, C. Sky Quality Meter measurements in a colour-changing world. *Monthly Notices of the Royal Astronomical Society* **2017**, *467*, 2966–2979. doi:10.1093/mnras/stx145.
90. Hänel, A.; Posch, T.; Ribas, S.J.; Aubé, M.; Duriscoe, D.; Jechow, A.; Kollath, Z.; Lolkema, D.E.; Moore, C.; Schmidt, N.; Spoelstra, H.; Wuchterl, G.; Kyba, C.C. Measuring night sky brightness: methods and challenges. *Journal of Quantitative Spectroscopy and Radiative Transfer* **2018**, *205*, 278–290. doi:10.1016/j.jqsrt.2017.09.008.
91. Cinzano, P. Night Sky Photometry with Sky Quality Meter. Technical Report 9, Istituto di scienza e tecnologia dell'inquinamento luminoso, 2007.
92. Den Outer, P.; Lolkema, D.; Haaima, M.; Hoff, R.v.d.; Spoelstra, H.; Schmidt, W. Intercomparisons of Nine Sky Brightness Detectors. *Sensors* **2011**, *11*, 9603–9612. doi:10.3390/s111009603.
93. Schnitt, S.; Ruhtz, T.; Fischer, J.; Hölker, F.; Kyba, C.C. Temperature Stability of the Sky Quality Meter. *Sensors* **2013**, *13*, 12166–12174. doi:10.3390/s130912166.
94. Den Outer, P.; Lolkema, D.; Haaima, M.; Van der Hoff, R.; Spoelstra, H.; Schmidt, W. Stability of the Nine Sky Quality Meters in the Dutch Night Sky Brightness Monitoring Network. *Sensors* **2015**, *15*, 9466–9480. doi:10.3390/s150409466.
95. Bará, S.; Lima, R.C.; Zamorano, J. Monitoring Long-Term Trends in the Anthropogenic Night Sky Brightness. *Sustainability* **2019**, *11*, 3070. doi:10.3390/su11113070.
96. Pun, C.S.J.; So, C.W. Night-sky brightness monitoring in Hong Kong. *Environmental Monitoring and Assessment* **2012**, *184*, 2537–2557. doi:10.1007/s10661-011-2136-1.
97. Zamorano, J.; García, C.; Tapia, C.; de Miguel, A.S.; Pascual, S.; Gallego, J. STARS4ALL Night Sky Brightness Photometer. *International Journal of Sustainable Lighting* **2017**, *18*, 49–54. doi:10.26607/ijsl.v18i0.21.
98. Bará, S.; Tapia, C.; Zamorano, J. Absolute Radiometric Calibration of TESS-W and SQM Night Sky Brightness Sensors. *Sensors* **2019**, *19*, 1336. doi:10.3390/s19061336.

99. Zamorano Calvo, J.; Sánchez de Miguel, A.; Nievas Rosillo, M.; Tapia Ayuga, C. NixNox procedure to build Night Sky Brightness maps from SQM photometers observations. ePrints Complutense 26982, Universidad Complutense de Madrid, Madrid, 2014.
100. Leinert, Ch..; Bowyer, S..; Haikala, L. K..; Hanner, M. S..; Hauser, M. G..; Levasseur-Regourd, A.-Ch..; Mann, I..; Mattila, K..; Reach, W. T..; Schlosser, W..; Staude, H. J..; Toller, G. N..; Weiland, J. L..; Weinberg, J. L..; Witt, A. N.. The 1997 reference of diffuse night sky brightness *. *Astron. Astrophys. Suppl. Ser.* **1998**, *127*, 1–99. doi:10.1051/aas:1998105.
101. Pilachowski, C.A.; Africano, J.L.; Goodrich, B.D.; Binkert, W.S. Sky brightness at the Kitt Peak National Observatory. *Publications of the Astronomical Society of the Pacific* **1989**, *101*, 707. doi:10.1086/132494.
102. Patat, F. The dancing sky: 6 years of night-sky observations at Cerro Paranal. *Astronomy & Astrophysics* **2008**, *481*, 575–591. doi:10.1051/0004-6361:20079279.
103. Grauer, A.; Brito, N. *Publications of the Astronomical Society of the Pacific* **2019**, *in press*.
104. Duriscoe, D.M.; Luginbuhl, C.B.; Moore, C.A. Measuring Night-Sky Brightness with a Wide-Field CCD Camera. *Publications of the Astronomical Society of the Pacific* **2007**, *119*, 192–213. doi:10.1086/512069.
105. Duriscoe, D.M. Photometric indicators of visual night sky quality derived from all-sky brightness maps. *Journal of Quantitative Spectroscopy and Radiative Transfer* **2016**, *181*, 33–45. doi:10.1016/j.jqsrt.2016.02.022.
106. Aceituno, J.; Sánchez, S.F.; Aceituno, F.J.; Galadí-Enríquez, D.; Negro, J.J.; Soriguer, R.C.; Gomez, G.S. An All-Sky Transmission Monitor: ASTMON. *Publications of the Astronomical Society of the Pacific* **2011**, *123*, 1076–1086. doi:10.1086/661918.
107. Bessell, M.S. UBVRI passbands. *Publications of the Astronomical Society of the Pacific* **1990**, *102*, 1181–1199. doi:10.1086/132749.
108. Linares, H.; Masana, E.; Ribas, S.J.; Gil, M.G.; Figueras, F.; Aubé, M. Modelling the night sky brightness and light pollution sources of Montsec protected area. *Journal of Quantitative Spectroscopy and Radiative Transfer* **2018**, *217*, 178–188. doi:10.1016/j.jqsrt.2018.05.037.
109. Falchi, F. Campaign of sky brightness and extinction measurements using a portable CCD camera. *Monthly Notices of the Royal Astronomical Society* **2010**, *412*, 33–48. doi:10.1111/j.1365-2966.2010.17845.x.
110. Rabaza, O.; Aznar-Dols, F.; Mercado-Vargas, M.; Espín-Estrella, A. A new method of measuring and monitoring light pollution in the night sky. *Lighting Research & Technology* **2014**, *46*, 5–19. doi:10.1177/1477153513510235.
111. Mohar, A. Mohar, A. Sky Quality Camera as a Quick and Reliable Tool for Light Pollution Monitoring. Proceedings of the International Conference on Light Pollution Theory, Modelling and Measurements, Jouvance, Québec, Canada, 26–28 May 2015, 2015, p. 47.
112. Kolláth, Z. Measuring and modelling light pollution at the Zselic Starry Sky Park. *Journal of Physics: Conference Series* **2010**, *218*, 012001. doi:10.1088/1742-6596/218/1/012001.
113. Kolláth, Z.; Dömény, A. Night sky quality monitoring in existing and planned dark sky parks by digital cameras. *International Journal of Sustainable Lighting* **2017**, *19*, 61–68. doi:10.26607/ijsl.v19i1.70.
114. Pascual, S.; Nievas, M.; Zamorano, J.; Contreras, J. PyASB, All Sky Brightness Pipeline. Proceedings of the Astronomical Data Analysis Software and Systems XXV, Sydney, Australia, 25–29 October 2015. Astronomical Society of the Pacific, 2017, Vol. 512, pp. 407–410.
115. Rosa Infantes, D. The Road Runner System. Presentation, IV International Symposium for Dark Sky Parks, Montsec, Spain, 2011.
116. Jechow, A.; Kolláth, Z.; Lerner, A.; Hänel, A.; Shashar, N.; Hölker, F.; Kyba, C.C. Measuring Light Pollution with Fisheye Lens Imagery from A Moving Boat – A Proof of Concept. *International Journal of Sustainable Lighting* **2017**, *19*, 15–25. doi:10.26607/ijsl.v19i1.62.
117. Jechow, A.; Ribas, S.J.; Domingo, R.C.; Hölker, F.; Kolláth, Z.; Kyba, C.C. Tracking the dynamics of skyglow with differential photometry using a digital camera with fisheye lens. *Journal of Quantitative Spectroscopy and Radiative Transfer* **2018**, *209*, 212–223. doi:https://doi.org/10.1016/j.jqsrt.2018.01.032.
118. Sánchez, S.F.; Aceituno, J.; Thiele, U.; Pérez-Ramírez, D.; Alves, J. The Night Sky at the Calar Alto Observatory. *Publications of the Astronomical Society of the Pacific* **2007**, *119*, 1186–1200. doi:10.1086/522378.

119. Massey, P.; Gronwall, C.; Pilachowski, C.A. The spectrum of the Kitt Peak night sky. *Publications of the Astronomical Society of the Pacific* **1990**, *102*, 1046. doi:10.1086/132733.
120. Massey, P.; Foltz, C.B. The Spectrum of the Night Sky over Mount Hopkins and Kitt Peak: Changes after a Decade1. *Publications of the Astronomical Society of the Pacific* **2000**, *112*, 566–573. doi:10.1086/316552.
121. Neugent, K.F.; Massey, P. The Spectrum of the Night Sky Over Kitt Peak: Changes Over Two Decades. *Publications of the Astronomical Society of the Pacific* **2010**, *122*, 1246–1253. doi:10.1086/656425.
122. Zhang, J.C.; Fan, Z.; Yan, J.Z.; Kumar, Y.B.; Li, H.B.; Gao, D.Y.; Jiang, X.J. The Night Sky Spectrum of Xinglong Observatory: Changes from 2004 to 2015. *Publications of the Astronomical Society of the Pacific* **2016**, *128*, 105004. doi:10.1088/1538-3873/128/968/105004.
123. Kyba, C.C.M.; Ruhtz, T.; Fischer, J.; Hölker, F. Red is the new black: how the colour of urban skyglow varies with cloud cover. *Monthly Notices of the Royal Astronomical Society* **2012**, *425*, 701–708. doi:10.1111/j.1365-2966.2012.21559.x.
124. Dobler, G.; Ghandehari, M.; Koonin, S.; Sharma, M. A Hyperspectral Survey of New York City Lighting Technology. *Sensors* **2016**, *16*, 2047. doi:10.3390/s16122047.
125. Alamús, R.; Bará, S.; Corbera, J.; Escofet, J.; Palà, V.; Pipia, L.; Tardà, A. Ground-based hyperspectral analysis of the urban nightscape. *ISPRS Journal of Photogrammetry and Remote Sensing* **2017**, *124*, 16–26. doi:10.1016/j.isprsjprs.2016.12.004.
126. Posch, T.; Binder, F.; Puschnig, J. Systematic measurements of the night sky brightness at 26 locations in Eastern Austria. *Journal of Quantitative Spectroscopy and Radiative Transfer* **2018**, *211*, 144–165. doi:10.1016/j.jqsrt.2018.03.010.
127. Kocifaj, M.; Lamphar, H.A.S.; Kundracik, F. Retrieval of Garstang's emission function from all-sky camera images. *Monthly Notices of the Royal Astronomical Society* **2015**, *453*, 819–827. doi:10.1093/mnras/stv1645.
128. Bortle, J.E. Introducing the Bortle Dark-Sky Scale. *Sky and Telescope* **2001**, *101*.
129. Kyba, C.C.M.; Wagner, J.M.; Kuechly, H.U.; Walker, C.E.; Elvidge, C.D.; Falchi, F.; Ruhtz, T.; Fischer, J.; Hölker, F. Citizen Science Provides Valuable Data for Monitoring Global Night Sky Luminance. *Scientific Reports* **2013**, *3*, 1835 EP –. doi:10.1038/srep01835.
130. Birriel, J.J.; Walker, C.E.; Thornsberry, C.R. Analysis of Seven Years of Globe at Night Data. *Journal of the American Association of Variable Star Observers* **2014**, *42*, 219–228.
131. Schroer, S.; Corcho, O.; Hölker, F. The impact of citizen science on research about artificial light at night. *Environmental Scientist* **2016**, *25*, 18–24.
132. Walker, M.F. Light Pollution in California and Arizona. *Publications of the Astronomical Society of the Pacific* **1973**, *85*, 508. doi:10.1086/129496.
133. Walker, M.F. The effects of urban lighting on the brightness of the night sky. *Publications of the Astronomical Society of the Pacific* **1977**, *85*, 508. doi:10.1086/130142.
134. Treanor, P.J. A simple propagation law for artificial night-sky illumination. *The Observatory* **1973**, *93*, 117–120.
135. Staude, H.J. Scattering in the Earth's Atmosphere: Calculations for Milky Way and Zodiacal Light as Extended Sources. *Astronomy and Astrophysics* **1975**, *39*, 325.
136. Garstang, R.H. Model for Artificial Night-Sky Illumination. *Publications of the Astronomical Society of the Pacific* **1986**, *98*, 364. doi:10.1086/131768.
137. Garstang, R.H. Night-sky brightness at observatories and sites. *Publications of the Astronomical Society of the Pacific* **1989**, *101*, 306–329. doi:10.1086/132436.
138. Aube, M.; Franchomme-Fosse, L.; Robert-Staehler, P.; Houle, V. Light pollution modelling and detection in a heterogeneous environment: toward a night-time aerosol optical depth retreival method. Atmospheric and Environmental Remote Sensing Data Processing and Utilization: Numerical Atmospheric Prediction and Environmental Monitoring; Huang, H.L.A.; Bloom, H.J.; Xu, X.; Dittberner, G.J., Eds. SPIE, 2005. doi:10.1117/12.615405.
139. Aube, M. Physical behaviour of anthropogenic light propagation into the nocturnal environment. *Philosophical Transactions of the Royal Society B: Biological Sciences* **2015**, *370*, 20140117–20140117. doi:10.1098/rstb.2014.0117.

140. Kerola, D.X. Modelling artificial night-sky brightness with a polarized multiple scattering radiative transfer computer code. *Monthly Notices of the Royal Astronomical Society* **2006**, *365*, 1295–1299. doi:10.1111/j.1365-2966.2005.09821.x.
141. Kocifaj, M. Light-pollution model for cloudy and cloudless night skies with ground-based light sources. *Applied Optics* **2007**, *46*, 3013. doi:10.1364/ao.46.003013.
142. Cinzano, P.; Falchi, F. The propagation of light pollution in the atmosphere. *Monthly Notices of the Royal Astronomical Society* **2012**, *427*, 3337–3357. doi:10.1111/j.1365-2966.2012.21884.x.
143. Kocifaj, M.; Lamphar, H.A.S. Angular Emission Function of a City and Skyglow Modeling: A Critical Perspective. *Publications of the Astronomical Society of the Pacific* **2016**, *128*, 124001. doi:10.1088/1538-3873/128/970/124001.
144. Kocifaj, M. Two-stream approximation for rapid modeling the light pollution levels in local atmosphere. *Astrophysics and Space Science* **2012**, *341*, 301–307. doi:10.1007/s10509-012-1074-x.
145. Kocifaj, M. Ground albedo impacts on higher-order scattering spectral radiances of night sky. *Journal of Quantitative Spectroscopy and Radiative Transfer* **2019**, *239*, 106670. doi:10.1016/j.jqsrt.2019.106670.
146. Kocifaj, M. Modeling the night-sky radiances and inversion of multi-angle and multi-spectral radiance data. *Journal of Quantitative Spectroscopy and Radiative Transfer* **2014**, *139*, 35–42. doi:10.1016/j.jqsrt.2013.12.002.
147. Kocifaj, M.; Lamphar, H.A.S. Skyglow: a retrieval of the approximate radiant intensity function of ground-based light sources. *Monthly Notices of the Royal Astronomical Society* **2014**, *439*, 3405–3413. doi:10.1093/mnras/stu180.
148. Kocifaj, M. Towards a comprehensive city emission function (CCEF). *Journal of Quantitative Spectroscopy and Radiative Transfer* **2018**, *205*, 253–266. doi:10.1016/j.jqsrt.2017.10.006.
149. Kocifaj, M.; Solano-Lamphar, H.A.; Videen, G. Night-sky radiometry can revolutionize the characterization of light-pollution sources globally. *Proceedings of the National Academy of Sciences* **2019**, *116*, 7712–7717. doi:10.1073/pnas.1900153116.
150. Kocifaj, M. Night sky luminance under clear sky conditions: Theory vs. experiment. *Journal of Quantitative Spectroscopy and Radiative Transfer* **2014**, *139*, 43–51. doi:10.1016/j.jqsrt.2013.12.001.
151. Duriscoe, D.M. Measuring Anthropogenic Sky Glow Using a Natural Sky Brightness Model. *Publications of the Astronomical Society of the Pacific* **2013**, *125*, 1370–1382. doi:10.1086/673888.
152. Fotios, S.; Gibbons, R. Road lighting research for drivers and pedestrians: The basis of luminance and illuminance recommendations. *Lighting Research & Technology* **2018**, *50*, 154–186. doi:10.1177/1477153517739055.